JOINT EUROPEAN TORUS

JET–P(93)70

T.E. Stringer

The Role of Radial Electric Field in the Plasma Edge Region

The Role of Radial Electric Field in the Plasma Edge Region

T.E. Stringer

JET-Joint Undertaking, Culham Science Centre, OX14 3DB, Abingdon, UK

Preprint of a paper presented at the 5th Workshop on
Magnetic Confinement Fusion: Plasma Boundary Physics in
Tokamaks and Stellarators
VIMP Santander, Spain, 23-27 August 1993.
September 1993

ABSTRACT

After a brief introduction to neoclassical transport, its role in determining the radial electric field in the presence of non-ambipolar loss mechanisms, such as fast ion orbit loss or magnetic stochasticity, will be discussed. This leads to plausible explanations for the L to H mode transition, and for the pump-out of impurities from the edge plasma during an ELM.

1. INTRODUCTION

There are several processes which can cause preferential loss of either ions or electrons. One which will be considered later is the loss of trapped ions whose orbits are wide enough to strike the limiter or enter a divertor. What produces the neutralising radial current, and how is it related to E_r?

Classical collisional diffusion, such as occurs in a cylinder, is always ambipolar. The transport produced by electrostatic fluctuations is ambipolar, or nearly so. This is because the ion and electron densities must be equal, while they share the same $\underline{E} \times \underline{B}$ drift velocity, apart from a small finite Larmor radius correction. It has frequently been stated that neoclassical (NC) fluxes are "automatically ambipolar", in which case they cannot carry a current either. Sec. 2 points out why this statement is not generally true.

Section 3 gives a somewhat oversimplified heuristic description of the NC loss process. Analytic expressions for the NC particle fluxes in the banana and plateau regimes are given in Section 4, and the special case where other loss processes are either absent or ambipolar is discussed. Section 5 briefly describes some measurements of the radial profile of potential and points out how magnetic stochasticity may reverse the sign of E_r.

Examples of ion orbits which enter the divertor are shown in Section 6, and an approximate estimate of the resulting ion loss current is described in Section 7. This current must be balanced by a NC current. This ambipolar condition determines Er. as discussed in Section 8. The variation of these two currents is such that, at some critical value of the orbit loss current, a bifurcation occurs, with a sudden increase in Er. This underlies the most popular explanation for the abrupt appearance of a large Er in the edge plasma during the L to H mode transition. The way such an electric field could reduce the fluctuations and hence improve the confinement, is described qualitatively in Section 9.

The NC transport of impurities is briefly summarised in Section 10, and impurity transport in a stochastic magnetic field is discussed in Section 11. This provides a plausible explanation for the observed pump-out of impurities from the edge plasma during ELMs.

It should be mentioned some of the conclusions put forward are still controversial, in particular that NC transport is not necessarily ambipolar.

2. WHY NEOCLASSICAL FLUXES ARE NOT GENERALLY AUTOMATICALLY AMBIPOLAR

I will first outline the usual derivation of automatic ambipolarity. It starts with the fluid momentum equation for the j^{th} species

$$n_j m_j \frac{d\underline{u}_j}{dt} = n_j e_j\left(\underline{E} + \underline{u}_j \times \underline{B}\right) - \nabla\, \underline{\underline{P}}_j + \sum\nolimits_k \underline{F}_{jk}\,. \quad (1)$$

where $\underline{F}_{jk}$ = collisional friction with the k^{th} species. All kinetic effects, such as trapped or resonant particles, are hidden in the pressure tensor $\underline{\underline{P}}_j$.

We now take the ϕ-component of this equation. To get rid of $\left(\nabla\, \underline{\underline{P}}_j\right)_\phi$ we first multiply by R, the distance from the axis of symmetry as shown in Fig. 1. Integrating this over a flux surface, $R(\nabla\, \underline{\underline{P}})_\phi$ dS is a perfect differential and so vanishes, giving

$$m_j\left\langle n_j \frac{du_{j\phi}}{dt} R\right\rangle = \left\langle n_j e_j E_\phi R\right\rangle + e_j \Gamma_j \bar{B}_\theta R_o + \left\langle \sum\nolimits_k F_{jk\phi} R\right\rangle.$$

where R_o is the radius of the minor axis, and angular brackets denote flux surface averaging. If we separate off the classical collisional and $\underline{E}\times\underline{B}$ fluxes, we get a relation for the neoclassical flux Γ^N

$$m_j\left\langle n_j \frac{du_{j\parallel}}{dt} R\right\rangle = \left\langle n_j e_j E_\parallel R\right\rangle + e_j \Gamma_j^N \bar{B}_\theta R_o + \left\langle \sum F_{jk\parallel} R\right\rangle \quad . \qquad (2)$$

Assuming a stationary equilibrium, the LHS of Eq. (2) is zero. When we sum over all species, the first term on the right vanishes, since $\sum n_j e_j = 0$. We thus get

$$R_o \bar{B}_\theta \sum e_j \Gamma_j^N = -\left\langle R - \Sigma_j \Sigma_k F_{jk\parallel} \right\rangle = 0. \qquad (3)$$

The sum of all friction terms must vanish, because momentum is conserved in the collisions ($F_{jk} = -F_{kj}$). Hence apparently momentum conservation forces the NC fluxes to be ambipolar, without having to invoke the quasi-neutrality condition.

The validity of the above analysis is limited by the tacit assumption that only collisional and NC processes occur. However, we know that anomalous transport and anomalous toroidal viscosity always occur experimentally. The radial current carried by the trapped ion orbit loss contributes a toroidal force $j_r^L B_\theta$ over the edge plasma. Anything which contributes toroidal momentum must be included in the flux surface averaged momentum equation.
Summing over all species now gives

$$\sum e_j \Gamma_j^N = \bar{j}_r \bar{B}_\theta + \left\langle \tilde{j}_r \tilde{B}_\theta \right\rangle + \text{anomalous viscous force.} \qquad (4)$$

Thus the NC fluxes are automatically ambipolar only in the idealised case where there is no other source of toroidal momentum [1]. In general NC fluxes **can** carry a net radial current and, as we shall see, play a major part in determining E_r.

3. INTRODUCTION TO NEOCLASSICAL TRANSPORT

a) Banana Regime

I consider the simplest tokamak geometry, with circular flux surfaces.

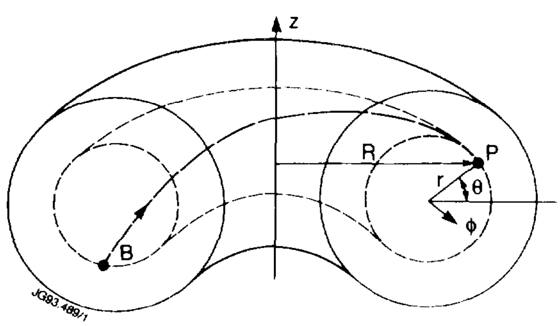

Fig. 1 The Toroidal Model

When there is a radial electric field, E_r, the poloidal rotation of a particle is

$$r\frac{d\theta}{dt} = \frac{B_\theta}{B}v_\parallel - \frac{E_r}{B} = \frac{B_\theta}{B}\left(v_\parallel - \frac{E_r}{B_\theta}\right).$$

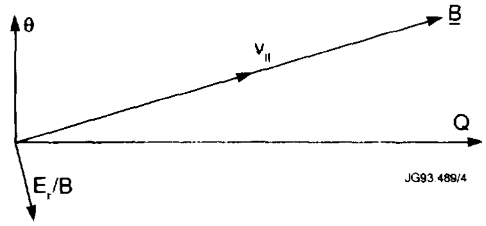

Particles with $v_\parallel \approx E_r / B_\theta$ rotate slowly. If the velocity at $\theta = 0$ lies in the velocity band

$$\left|v_\parallel - \frac{E_r}{B_\theta}\right| < v_\perp\sqrt{2\frac{r}{R_o}} \tag{5}$$

the particle is reflected by the stronger magnetic field on the inboard side, and bounces to and fro in a trapped orbit, as illustrated in Fig. 2. The radial width of the orbit, resulting from the vertical ∇B and curvature drifts, is approximately $\varepsilon^{1/2}\rho_{j\theta}$, where $\varepsilon \equiv r / R_o$ and $\rho_{j\theta}$ is the Larmor radius in the poloidal magnetic field.

The radial particle flux results from the abrupt changes in mean orbit radius, which occur when particles are collisionally scattered from circulating into trapped orbits, or vice versa. Suppose a particle enters the trapped velocity band at point P. Its orbit changes to a banana, which lies inside or outside its original magnetic surface depending on whether $u = v_\parallel - E_r / B_\theta$ is initially positive or negative. Thus the orbit displacement has the opposite sign to u, and a magnitude which decreases as the trapping point moves further from P. Conversely, when a particle is scattered out of the trapped velocity band, its orbit displacement has the same sign as u.

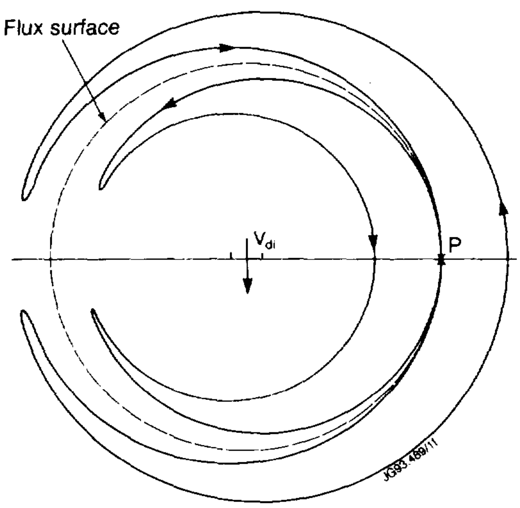

Fig. 2 Trappd ion orbits

The net diffusion depends on the difference in the number of particles which are trapped and detrapped at the two edges of the trapped velocity band. The analysis is too long to reproduce here, but an approximate physical picture is as follows:

To first order the inward and outward displacements cancel. In next approximation, a net flux results from the small variation in particle distribution function around a magnetic surface. Just outside the trapped band, the variation in velocity distribution function is like

$$\tilde{f}(r,\theta,\ \underline{v}) \sim \frac{\varepsilon}{u}\left(v_{\parallel}^2 + \frac{v_{\perp}^2}{2}\right) G\left(\frac{E_r}{B_\theta}\right)\cos\theta \tag{6}$$

where $G(v_{\parallel}) = -\dfrac{\partial f_o}{\partial v_{\parallel}} - \dfrac{1}{\Omega_{j\theta}}\dfrac{\partial f_o}{\partial r}$, and $\Omega_{j\theta} = e_j B_\theta / m_j$.

The product of f with the orbit displacement, when averaged over velocity and poloidal angle, yield the usual NC flux, apart from a numerical factor.

b) Plateau Regime

Banana orbits occur only at rather low collision frequencies, when the collisional mean free path

$$\lambda_{mfp} > qR\left(\frac{R}{r}\right)^{3/2}.$$

At higher collision frequencies a particle is scattered out of the trapped velocity band before it has time to complete a banana orbit.

Those particles which have $v_{\parallel} \approx E_r / B_\theta$ still have a slow poloidal rotation, and hence the radial component of their ∇B drift is steady. Effectively they complete part of a banana orbit. Because of their relatively large radial displacements, these resonant particles dominate the radial particle flux.

Since the vertical ∇B drift carries particles outwards in the lower half plane, and inwards in the upper half plane, as shown in Fig. 3 the net flux depends on the difference in resonant particle density at the top and bottom. This is proportional to

$$\propto -\left(v_{Dj} \frac{\partial f_o}{\partial r} + \frac{dv_{\parallel}}{dt} \cdot \frac{\partial f_o}{\partial v_{\parallel}} \right)$$

$$\propto -\left(\frac{\partial f_{oj}}{\partial v_{\parallel}} + \frac{1}{\Omega_{j\theta}} \frac{\partial f_{oj}}{\partial r} \right)_{v_{\parallel} = \frac{E}{B_\theta}} \sin\theta$$

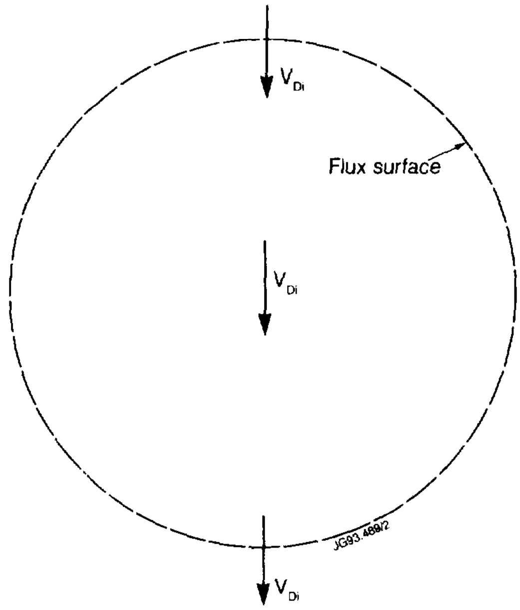

Fig. 3 Resonant Particle Drift

This is the same function as arose in the banana regime.

4. Results of the Neoclassical Analysis

Banana and plateau diffusion were first studied by Galeev and Sagdeev [2]. For arbitrary values of E_r and $\bar{v}_{j\parallel}$ they derived fluxes in the form

$$\Gamma_j = -D_j n \left[\frac{n'}{n} + \gamma \frac{T_j'}{T_j} - \frac{e_j}{T_j}\left(E_r - B_\theta \bar{v}_{j\parallel}\right) \right] \exp\left[-\left(\frac{E_r - B_\theta \bar{v}_{j\parallel}}{B_\theta v_{tj}} \right)^2 \right] \qquad [7]$$

where a dash denotes differentiation with respect to r and $v_{tj} = \sqrt{2T_j / m_j}$.

In the banana regime, where $\lambda_{mfp} > qR(R/r)^{3/2}$,

$$D_j = 1 \cdot 12 \upsilon_j \rho_{j\theta}^2 \quad , \quad \gamma = -0.17 \qquad [8]$$

where $\upsilon_j = \Sigma_k \; \upsilon_{jk}$ is the collision frequency, and $\rho_{j\theta} = v_{tj} / \Omega_{j\theta}$.

In the plateau regime, where $qR < \lambda_{mfp} < qR(R/r)^{3/2}$

$$D_j = \frac{\sqrt{\pi}}{4}\left(\frac{r}{R}\right)^2 \frac{\rho_{j\theta}^2}{r}\frac{B_\theta}{B}\cdot v_{tj} \quad , \quad \gamma = \frac{3}{2}. \qquad [9]$$

The variation in the diffusivities, D_i and D_e with collision frequency is sketched in Fig. 4

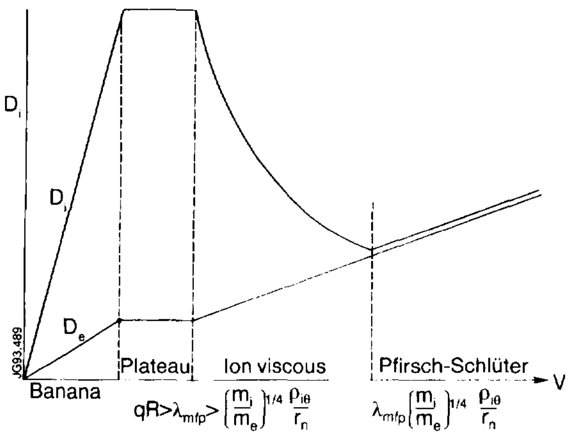

Fig. 4 Variation in the neoclassical diffusivities with collision frequency

In both plateau and banana regimes the coefficient in the ion equation

$$D_i \sim \left(\frac{m_i}{m_e}\right)^{1/2} \times D_e.$$

When $\left(\frac{m_e}{m_i}\right)^{1/4} \frac{\rho_{i\theta}}{r_n} < \lambda_{mfp} < qR$, the ion diffusion is dominated by parallel ion viscosity. When $\lambda_{mfp} < \left(\frac{m_e}{m_i}\right)^{1/4} \frac{\rho_{i\theta}}{r_n}$, we enter the Pfirsch-Schlüter regime where resistivity is dominant.

The NC radial current is dominated by the ions, $j_r^N = e\Gamma_i^N$, where Γ_i^N is given in Eq. 7. This defines the NC radial conductivity.

When there is no other transport, or the other transport process is itself ambipolar (as for electrostatic turbulence), then j_r^N must $= 0$. This determines the ambipolar electric field

$$E_r - B_\theta \bar{v}_{i\|} = \frac{T_i}{e}\left[\frac{n'}{n} + \gamma\frac{T_i'}{T_i}\right]. \qquad [10]$$

The ion poloidal fluid velocity is then

$$-\frac{E_r}{B} + \frac{B_\theta}{B}\bar{v}_{i\|} + \frac{1}{neB}\frac{dP_i}{dr} = (1-\gamma)\frac{T_i'}{eB}.$$

Many authors prefer to use the fluid form of the equations, where trapped and resonant particle effects are all hidden in the viscous term $\left(\nabla \underline{\underline{P}}_j\right)$. They attribute the above partial cancellation of the diamagnetic velocity to "damping of the poloidal rotation by NC viscosity", which give no clue to the physical mechanism.

From the kinetic analysis one sees how the ions reduce their flux to balance the electrons. The initially larger ion loss causes a negative E_r to grow. This reduces the poloidal variation in the density of ions entering the trapped velocity band

$$\tilde{f}(r,\theta,v) \propto G\left(\frac{E_r}{B_\theta}\right) \approx \left[-\frac{\partial f_o}{\partial v_\|} - \frac{1}{\Omega_{j\theta}}\frac{\partial f_o}{\partial r}\right]_{v_\|=E_r/B_\theta}$$

and hence reduces the ion flux. At some E_r, where the terms in G nearly cancel, the ion flux becomes equal to the electron flux. The growth in E_r then ceases.

If NC transport were "automatically ambipolar", then Eq., (10) must always be satisfied to ensure $\Gamma_i = \Gamma_e$. Most earlier analysis used this relation to eliminate $E_r - B_\theta \bar{V}_{i\|}$ from Eq. (7), thus obtaining a NC flux which is independent of Er. As shown in Sec. 2, the argument for automatic ambipolarity is valid only when there is no other source of toroidal momentum. Eq. [7] is the general form, which applies in all conditions.

5. EXPERIMENTAL EVIDENCE FOR THE NEOCLASSICAL E_r

Measurements of E_r inside the limiter radius or separatrix are usually consistent with this NC prediction. This supports the view that anomalous transport is due to electrostatic fluctuations. Since these are nearly ambipolar, they do not influence E_r. During strong MHD activity, however, the measured E_r may change to outwards. This is because in a stochastic magnetic field, electrons can escape along field lines more rapidly than the NC ion flux, and so a positive E_r is needed to restrain them. The same thing happens in an edge plasma with ergodic magnetic limiter.

The above behaviour can be seen in the potential profiles measured in TEXT [3]. The dashed curve in Fig. 5 shows a typical profile, without the ergodic magnetic limiter (EML). E_r is inwards until one enters the limiter shadow. In the scrape-off-layer, E_r is determined by ion and electron flows along the magnetic field, and is always outwards.

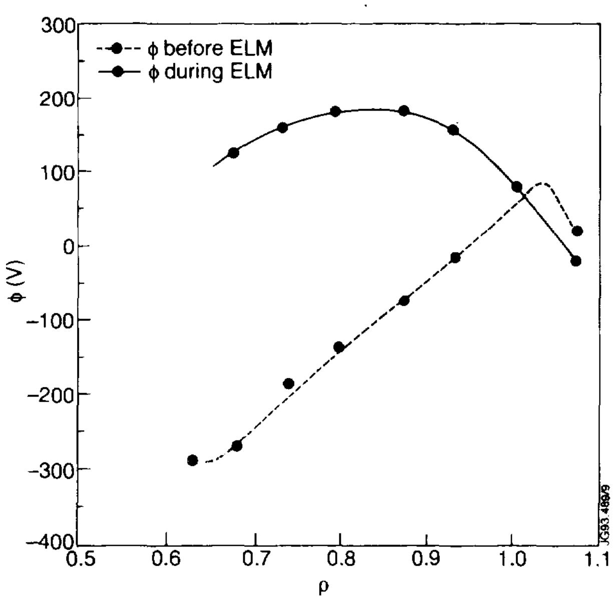

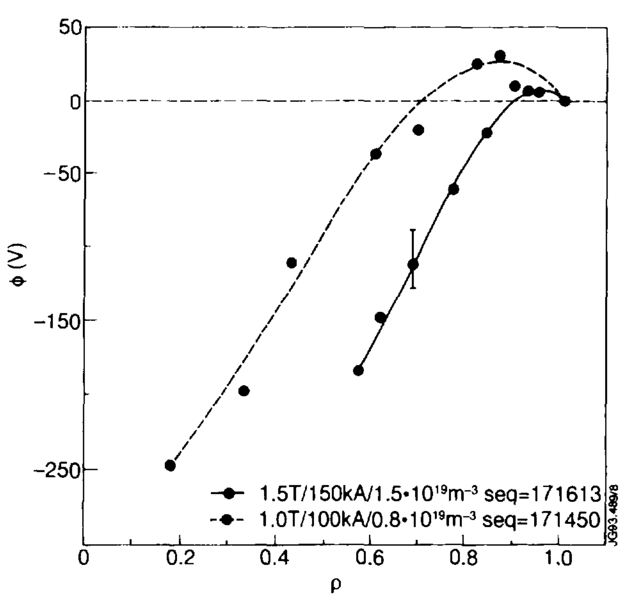

Fig. 5: Potential profiles in TEXT with and without EML [3].

Fig. 6: Potential profiles in TEXT when MHD activity is strong [3].

The solid curve is the potential after the EML is turned on. E_r is now positive over the outer 15% of the radius. This corresponds to the region over which the magnetic field is calculated to be stochastic.

The magnetic fluctuations in TEXT are usually weak, but in a specific parameter range they are unusually large. Fig. 6 shows the potential profiles for two such cases. The region where E_r is positive again agrees with the calculated region over which magnetic island chains overlap. Thus spontaneous magnetic fluctuations have a similar effect to the perturbation generated externally by the EML. In MHD quiescent conditions, the measured E_r is consistent with the usual

NC value. Where the magnetic field is stochastic, however, E_r is positive, which is consistent with overall ambipolarity.

6. ION ORBIT LOSS FROM THE EDGE PLASMA

This is an example of a process which can change the ambipolar electric field. We saw earlier that ions with $v_{\parallel} \approx E_r/B_\theta$ become trapped in the magnetic field. Their bounce orbits have relatively large excursions around their mean magnetic surface. Near the plasma edge these orbits may strike the limiter, or enter a divertor.

Two loss orbits in JET, computed by Chankin and McCracken [4], are shown in Fig. 7. In Fig. 7a the ion enters the divertor after being reflected. Fig. 7b shows an energetic ion which is lost before reaching the inboard side.

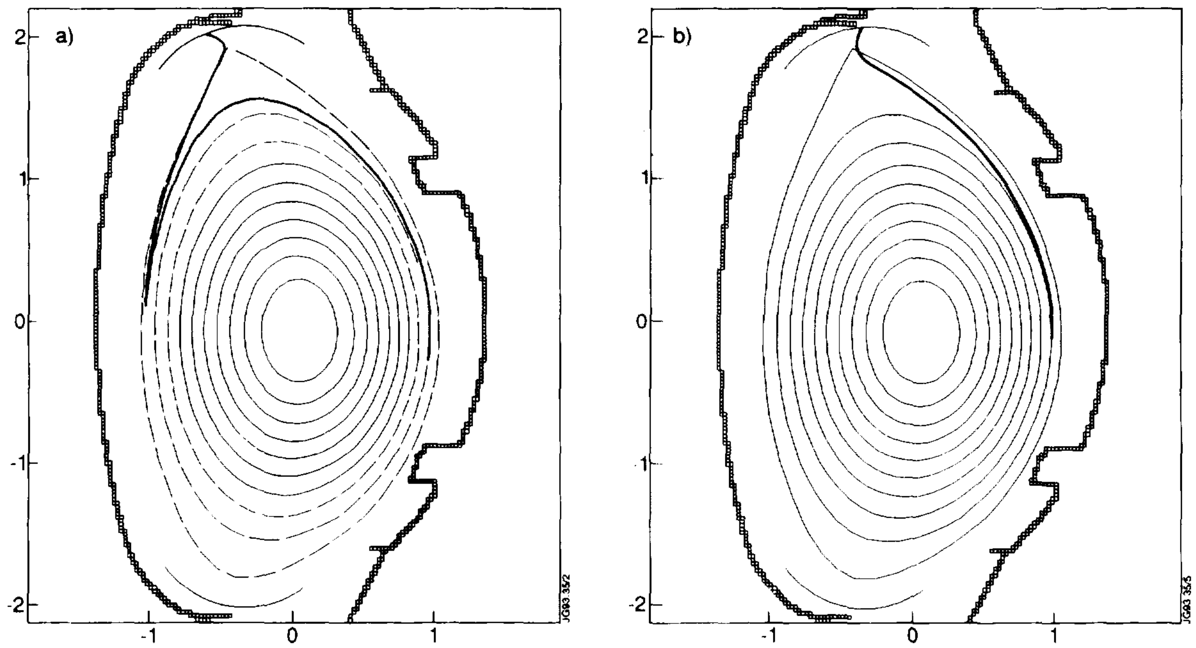

Fig. 7 Computed Ion Loss Orbits in JET [4].

Since the orbit width $\propto$ (kinetic energy $\times$ mass)$^{1/2}$, energetic ions are lost first, and the electron orbit loss is negligible.

7. ESTIMATED ION ORBIT LOSS FROM THE EDGE PLASMA

Any ion scattered into the trapped velocity band within a distance ~ $\varepsilon^{1/2}\rho_{i\theta}$ from the separatrix is likely to enter the divertor. To be trapped, an ion must have $v_{||} \approx E_r/B_\theta$, and collision frequency low enough to complete a banana orbit,

$$\text{i.e.} \quad \frac{v}{v_{ti}} > (\nu_{i*})^{1/4} \text{ where } \nu_{i*} = \frac{\bar{\nu}_i}{\varepsilon^{3/2}}\frac{qR}{v_{ti}} = \frac{qR}{\lambda_{mfp}} \cdot \frac{1}{\varepsilon^{3/2}}.$$

The rate of ion loss was estimated by Shaing and Crume [5] as follows.

$$\frac{dN}{dt} = \text{Ion loss/unit surface area}$$

$$= \text{collision frequency} \times \text{density of trapped ions} \times \text{width of loss layer}$$

$$\sim \bar{\nu}_i n \exp\left[-\left\{\left(\frac{E_r}{B_\theta v_{ti}}\right)^4 + \nu_{i*}\right\}^{1/2}\right]\varepsilon^{1/2}\rho_{i\theta}\left[\left(\frac{E_r}{B_\theta v_{ti}}\right)^4 + \nu_{i*}\right]^{-1/2} \tag{11}$$

The variation in dN/dt with E_r is sketched in Fig. 8.

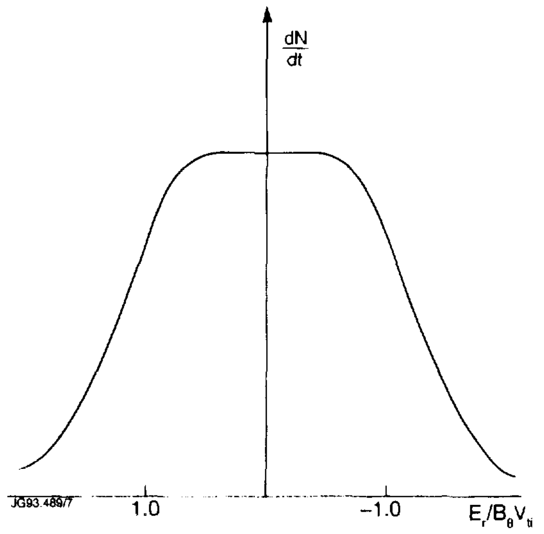

Fig. 8

The decrease with increasing E_r results from the decrease in trapped ion density as the trapped velocity band, $v_{||} \approx E_r/B_\theta$ is pushed out to the Maxwellian tail. The ν_{i*} dependence removes those ions which are too collisional to be trapped.

8. BIFURCATION IN THE ELECTRIC FIELD PROFILE AT LH TRANSITION

Simultaneously with the transition to H-mode confinement, a large inward $E_r \sim O$ (10kV/m) suddenly appears in the outer few centimeters of plasma [6]. Several different explanations have been proposed for how this electric field is set up. In the most popular explanation, proposed by Shaing and co-workers [5], the charge loss due to ion orbits entering the divertor must be balanced by a neoclassical radial current flow.

In the plateau regime, the NC current is

$$j_r^N = -neD_i\left[\frac{n'}{n}+\frac{3}{2}\frac{T_i'}{T_i}-\frac{e}{T_i}\left(E_r - B_\theta \bar{v}_{i\parallel}\right)\right]\exp\left[-\left(\frac{E_r - B_\theta \bar{v}_{i\parallel}}{B_\theta v_{ti}}\right)^2\right] \qquad [12]$$

This varies with E_r like curve (a) below

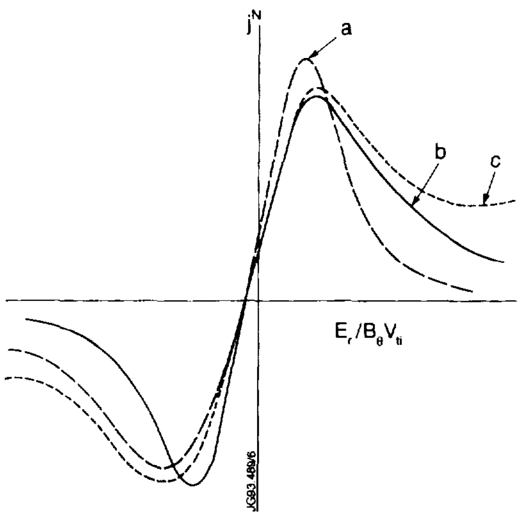

Fig. 9 Variation in NC current with $E_r / B_\theta v_{ti}$

In a typical edge plasma, parallel ion viscosity becomes important when $E_r/B_\theta v_{ti} > 1$, where the density of resonant particles is low. This increases the plasma current, as illustrated by curve (b). Charge exchange collisions with neutrals gives rise to a current proportional to rotation velocity, i.e. $\propto E_r$ [7]. Its inclusion is illustrated by curve (c).

The electric field is determined by the ambipolar condition $j^L(E_r)+j^N(E_r)=0$.

We can see the solution pictorially by plotting j^L and $-j^N$, and noting where they intersect. Fig. 10 illustrates such plots for three different conditions, with temperatures increasing from (a) to (c). In Fig 10a there is one intersection, the ambipolar E_r being comparable with the standard neoclassical value. As temperature increases the fast ion loss increases. In Fig 10b there are three possible ambipolar E_r. The middle one is unstable. From continuity, E_r is given by the intersection closest to the origin. In Fig 10c the two lowest intersections have vanished, and there is only one possible ambipolar E_r, which is $> v_{ti}B_\theta$. Curves (a) and (b) correspond to L-mode plasmas, and (c) to an H-mode. When the two lowest intersections disappear, we expect a sudden large increase in the negative electric field over an edge layer of width $\sim \rho_{i\theta}$. This is what is observed.

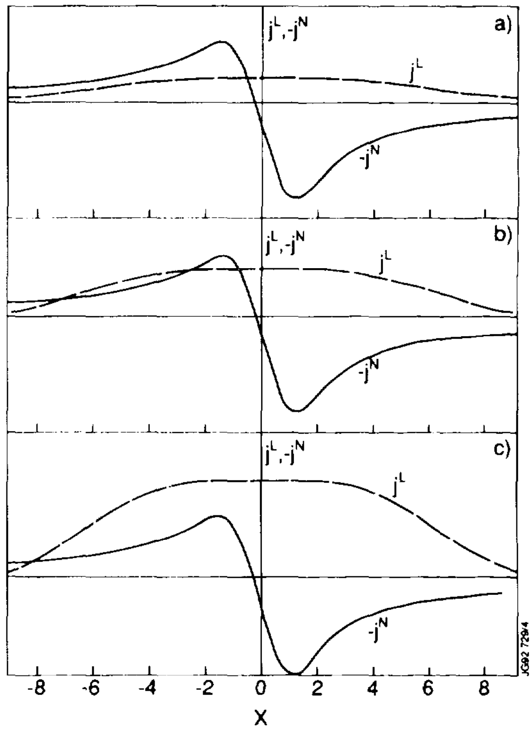

Fig. 10 Variation in NC and ion loss currents with $x = E_r/B_\theta v_{ti}$

9. STABILISATION OF FLUCTUATION BY dE_r/dr

The measured fluctuations in the H-mode are significanly lower than in the preceding L-mode, suggesting that the associated reduction in anomalous transport is responsible for the improved confinement. Can the large electric field be responsible for the reduced fluctuations?

A strong gradient in Er produces strong shear in the $\underline{E}$ x $\underline{B}$ drift velocity. This tears apart the coherent cellular pattern of the unstable modes [8], as illustrated in Fig.11.

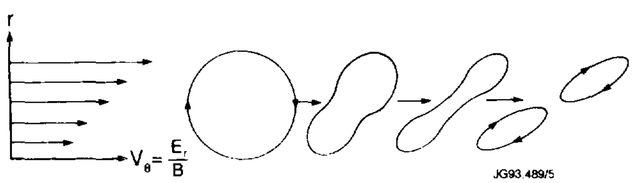

Fig. 11 Effect of Sheared Flow on a Convective Cell.

This effect can be expressed by a decorrelation time

$$\tau_c \propto 1/(dv_\perp/dr).$$

If this is less than the decorrelation time due to the background diffusion, $\tau_c \sim D/\lambda^2$ (where λ = length scale), then the sheared flow reduces the nonlinear saturation level of fluctuations.

Thus a plausible complete explanation for the L-H transaction is

i) When the ion orbit loss becomes large enough, ambipolarity forces E_r in the edge plasma to jump to a larger value.

ii) The shear in E_r then reduces the fluctuation level, and hence the anomalous transport.

10. NEOCLASSICAL TRANSPORT OF IMPURITIES

The neoclassical impurity flux can be written in the same form as the main plasma flux. In the banana regime the flux of the a^{th} species is [9].

$$\Gamma_a^N = 1.46 \ \epsilon^{1/2} \ \nu_a \rho_{a\theta}^2 n_a \left[-\frac{n'_a}{n_a} - \gamma_a \frac{T'}{T_a} + \frac{Z_a e}{T_a}\left(E_r - B_\theta \bar{v}_{a\parallel}\right)\right] \quad (13)$$

when $\nu_a = \Sigma_b \nu_{ab}$ is the collision frequency. Note that, because E_r is multiplied by the atomic charge, impurities are more sensitive to the radial electric field.
When only NC transport occurs, an inward E_r is still necessary to reduce the ion loss to that of the slower diffusing electrons. Because this inward E_r has a stronger effect on impurities, they move inwards, to become strongly peaked on axis.

The ambipolar E_r is not affected by electrostatic fluctuations, since they produce ambipolar diffusion. However, the anomalous impurity diffusion reduces the peaking on axis. If the impurities have time, they reach a steady state given by

$$\frac{n_a(r)}{n_a(o)} \sim \left[\frac{n_i(r)}{n_i(o)}\right]^\alpha \ , \quad \alpha = \frac{Z_a D_N}{D_N + D_{an}}. \quad (14)$$

Although usually $D_{an} >> D_N$, when Z_a is large, $\alpha > 1$ and the impurity is more peaked than the main species, though much less so than if there is no anomalous transport.

11. IMPURITY TRANSPORT IN A STOCHASTIC MAGNETIC FIELD

In a stochastic magnetic field the radial electric field is determined by the ambipolar condition

$$\sum_a n_a Z_a D_a \left[-\frac{n'_a}{n_a} + \gamma_a \frac{T'_a}{T_a} + \frac{Z_a e}{T_a}\left(E_r - B_\theta \bar{v}_{a\parallel}\right) \right] = \Gamma_e^{an}(E_r) + \Gamma_e^N$$

where Γ_e^{an} is now the electron flow along stochastic field lines.

If stochasticity is strong, an outward E_r is needed to restrain the electron escape, as shown by the TEXT measurements discussed earlier. This increases the main ion loss rate but, because of the Z_a factor, the impurity loss rate is increased much more.

If short periods of strong MHD activity are separated by longer quiescent periods, when only electrostatic fluctuations are present, the following behaviour is expected. During the quiescent MHD periods, impurities should accumulate in the centre. This accumulation will be reversed during periods of magnetic stochasticity, when E_r is likely to be reversed. This causes a modest increase in the main ion loss rate, and a much more rapid loss of impurity.

Several examples where impurities were observed to accumulate on axis during MHD quiescent phases, and were then expelled during periods of MHD activity, are given in Ref. [11]. A similar behaviour in the edge plasma is observed during an ELM (Edge Localised Mode). Here the magnetic fluctuations are localised near the plasma edge, and so we might expect impurities to be ejected from this region only. This is exactly what is observed, as illustrated, for example in Fig. 12. This shows the time behaviour of H^α, electron density, and nickel radiation during an ELM-y H-mode in DIII-D [10].

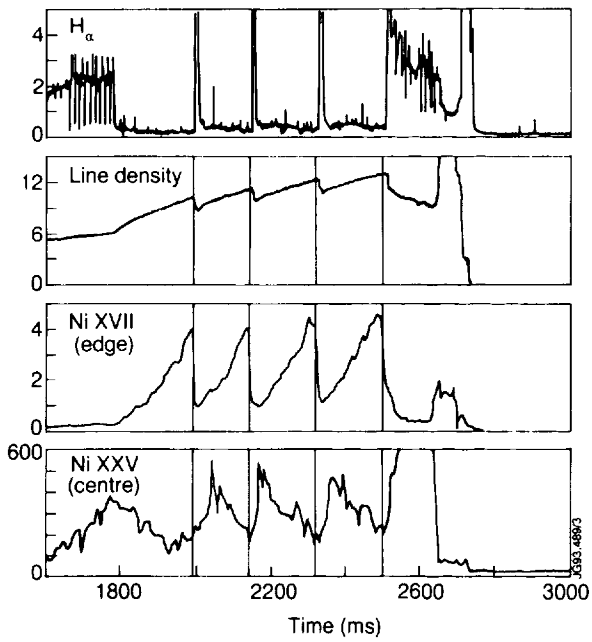

H^{α} spikes mark the occurrence of an ELM

$\bar{n}_e$ shows 0(20%) reduction during each ELM

Ni XVII, which radiates near edge, is reduced by factor 3

Ni XXV, which radiates from centre, shows no change during ELM

Fig. 12 Variation in H^{α}, N_e And N_i Radiation During Elms in DIII-D [10]

The variation in the central Ni density can be explained by anomalous plus neoclassical transport. Between ELMs, $n_e(r)$ becomes progressively more hollow and the NC convection forces the impurity profile to follow this hollowness. The sharp drop in the edge impurity during an ELM is just what is expected, due to stochastisation of the magnetic field and reversal of E_r near the edge.

12. SUMMARY

(i) The usual demonstration that neoclassical transport is automatically ambipolar is invalid when any other source of toroidal momentum is present, e.g. net radial current, anomalous viscosity, or magnetic stochasticity.

(ii) The neoclassical particle flux, derived by kinetic analysis, is a function of the radial electric field. E_r is then determined by imposing the ambipolar condition on the total particle flux.

(iii) Balancing the NC current flow against the ion orbit loss current provides a plausible explanation for the sudden appearance of a strong E_r over the plasma edge region. Stabilisation of the fluctuations by shear in the $\underline{E} \times \underline{B}$ rotation can then explain the improved H-mode confinement.

(iv) The maximum ion NC flux is $0\left(\frac{m_i}{m_e}\right)^{1/2}$ x max. electron NC flux, while the maximum electron loss along a stochastic magnetic field is 0 $(m_i/m_e)^{1/2}$ x max. ion loss. The electron stochastic loss can be balanced by the ion NC flux. When stochasticity is strong, the ambipolar E_r is outwards.

(v) Because of their high Z, impurity NC flux is more strongly affected by this change in E_r. Magnetic stochasticity is expected to produce pump-out of impurities with a much smaller reduction in main plasma density. Just such behaviour is observed in the edge plasma during an ELM.

REFERENCES

1. T.E. Stringer, Nuc. Fusion 32, 1421 (1992).

2. A.A. Galeev, R.Z. Sagdeev, Sov. Phys - JETP 26, 233 (1968).

3. X.Z. Yang, B.Z. Zhang, A.J. Wooton, P.M. Schoch, et al., Phys. Fluids B 3 3448, (1991).

4. A. Chankin, G. McCracken, JET-P (93) 25, submitted to Nuc. Fusion.

5. K.C. Shaing, E.C. Crume, Phys. Rev. Lett. 63, 2369 (1989).

6. R.J. Groebner, K.H. Burrell, K.H. Seraydarian, Phys. Rev. Lett. 64, 3015 (1991).

7. J. Cornelis, R. Sporkleen, G. van Oost, R.R. Weynants, submitted to Nuc. Fusion (1993).

8. H. Biglari, P.H. Diamond, P.W. Terry, Phys. Fluids B 2, 1 (1990).

9. J.W. Conner, Pl. Phys. 15, 765 (1973).

10. M.E. Perry et al., Nuc. Fusion 31, 1859 (1991).